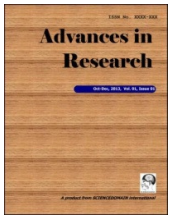

Advances in Research
3(4): 427-444, 2015, Article no.AIR.2015.038
ISSN: 2348-0394

SCIENCEDOMAIN *international*
www.sciencedomain.org

Groin Opening Effect on Shoreline

M. Balah[1], G. Elsaeed[2*], A. Eldegwy[3] and M. Hasan[2]

[1]Department of Civil Engineering, Faculty of Engineering, Suez Canal University, Ismailia, Egypt.
[2]Department of Civil Engineering, Faculty of Engineering, Shobra, Banha University, Cairo, Egypt.
[3]Department of Irrigation and Hydraulics, Faculty of Engineering, Cairo University, Cairo, Egypt.

Authors' contributions

This work was carried out in collaboration between all authors. All authors read and approved the final manuscript.

Article Information

DOI: 10.9734/AIR/2015/13379
Editor(s):
(1) Martin Kröger, Computational Polymer Physics Swiss Federal Institute of Technology (ETH Zürich) , Switzerland.
Reviewers:
(1) Wen-Cheng Liu, Department of Civil and Disaster Prevention Engineering, National United University, Taiwan.
(2) Anonymous, Hong Kong Polytechnic University, China.
Complete Peer review History: http://www.sciencedomain.org/review-history.php?iid=756&id=31&aid=6988

Original Research Article

Received 14th August 2014
Accepted 4th November 2014
Published 18th November 2014

ABSTRACT

An actual scale model of a groin was designed and constructed to investigate the impact of the gap width on the shoreline changes in the close vicinity of the groin. The Surface water Modeling System (SMS) model has been used to simulate the wave hydrodynamics around the groin for about 5 years to study the impact of the proposed groin on the shoreline and wave conditions at various time steps. The model has been calibrated and validated against the collected and measured field data. The dominant wave/current conditions along the North-West coast of Egypt have been considered for various possible configurations of the semi-open groin to identify the appropriate design. Wind and wave data of the El-Dekhila port Meteorological Station (EMS) have been adopted for the period 2010-2014.

The results and analysis provide general guidelines for the use of groins with a clear opening in coastal resorts that can be applied to a wide range of wave climates. It has also been found that a groin with a clear opening can help to provide safe swimming conditions with minimum impact on the shoreline if groins were properly studied. Wide gap spacing and permeable groins generally reduce the shoreline changes. It is found that the maximum erosion and accretion depths are almost equal in case of S>0.15 Lg for the cases investigated (Lg is the groin length, S is the gap width). The effective length on the up-drift side is much more than that on the down-drift for the cases investigated in this work. The up-drift is affected up to twice the length of the groin in case of no gap and the length is about 1.1 Lg in case of gap width equaling 0.15 Lg. The variation of the

**Corresponding author: Dr. Gamal Elsaeed - E-mail: gelsaeed@feng.bu.edu.eg;*

effective length on the down-drift varies slowly as the gap width varies. The effective length varied from 1.2 to 1.1 as S/Lg varies from 0 to 0.15. It is noteworthy that the variation of the effective length is nearly linear with the gap width in this study.

Keywords: Groin; shoreline changes; coastal hydro-dynamics; numerical models; Egyptian coast; environmental impacts and Shoreline changes.

1. INTRODUCTION

Problems of erosion experienced along the coast at present are not due to natural phenomena, but due to the action of man such as the noticeable impact of the development of the Alexandria corniche. One of the problems facing the development of the Alexandria corniche is the degradation of sandy beaches through widening the existing road and placing concrete blocks. Such works have led to alteration of beach dynamics and thus a loss of beach materials. Another problem is storm waves during the winter season. These storms cause the beach material to be blown from the beach and to be deposited on the road. During these storms large sections of the corniche seawall were breached and parts of the corniche behind washed away. Significant voiding behind was also discovered which apparently undermined sections of the corniche seawall.

The Ministry Of Housing in Egypt studied morphological and water components in the El-Alemein marina resort [1]. It studied the use of groins, detached breakwaters and sand bypass/nourishment as protection measures for the erosion problems encountered. It was recommended to protect the shoreline using a system of groins combined with an initial amount of nourishment.

The use of groins for protecting the beach was applied in many places worldwide, but it still has the adverse impact of accretion/erosion as well as poor water quality at stagnation points. Groins with a clear opening or permeable groins could be one of the possible protection structures, which can be used to protect the shore from erosion with minor environmental impact, especially if attention is given to their design. Groins have several advantages; e.g., low cost, easy to construct, do not impair aesthetic amenity of the beach, effective control on erosion, retain sand on a beach and less adverse impact on the environment.

Almost no reliable studies have been conducted on the use of groins with a clear opening along the Egyptian coast for protecting the beaches while limiting shoreline changes to a minimum. The internal properties of the groin, the number, size and location of the openings can be of paramount impact on the shoreline changes and water circulation as well. This study focuses on the use of a groin with a clear opening and tests the appropriate size of the opening located at the center of the groin as well as the internal properties of the groin. The impact of the various designs of the groin on the shoreline changes, wave height distribution and radiation stresses have been investigated and guidelines have been summarized.

2. STUDY AREA

Delft hydraulics divided the Egyptian northern coastline into a number of cells based on the shape of the shoreline and the main head lands [2]. The cell is defined as a unit in which the long shore morphological interaction is anticipated to be relatively strong. The cell is bound by physical boundaries, e.g., rock head lands or harbors, such that interruption of long shore current takes place. The study area is located in cell (5). This area extends from El-Dikheila in the east to Ras El-Shaqiq in the west. This part of the coast is characterized by a chain of tourist villages and beautiful recreational beaches such as Marina village, Green, Marballa, Suez Canal village, Al-Hamam, Selsabil, Haydi, Ghernatah, Marakia, Burg Elarab and Sidi Krir. The pilot area is the coast of a new tourist resort located at Sidi Krir, kilometers 39.774/40.078 west of Alexandria along the Egyptian Northwestern Mediterranean coast, as illustrated in (Fig. 1).

The project area has a shoreline of nearly 300m and the approved design has one shore parallel submerged breakwater and two submerged groins. The crest of both the breakwater and the groins were set at -0.5m below Mean Sea Level (MSL). The submerged breakwater is located at 125m offshore the existing shoreline at an average water depth of 3.25m and having a length of 200m. The tidal range as recorded by the Al-Dikheila metrological station is less than 0.5 m. Two submerged groins are constructed normal to the shoreline connecting the

submerged breakwater with the shore parallel breakwater. The breakwater is centered in the shoreline such that 50 m are left on the west and east borders of the resort. The shoreline makes an angle of 40° with the North direction and by analyzing the wave rose at the area, it could be concluded that the predominant wave is perpendicular to the shoreline approximately. So, the slope of the seabed within the surf zone is about 35 (horizontal): 1 (vertical) causing a steep beach profile and hence strong rip currents. The area has long been suffering from rip currents as large as 1.0 m/sec and a limited safe swimming strip of less than 40 m during the prevailing wave conditions in the summer season as will be shown by the numerical model as well.

In May 2009 a bathymetric survey was carried out between levels of approximately ESAD-16 m and ESAD+3 m (Egyptian Survey Authority Datum, ESAD = 0.08 m below MSL). The bathymetry area, implemented for modeling covered an area of 3 km alongshore and 1.5 km offshore, as shown in (Fig. 2). This area covered a distance of 1500 m on both sides of the center of the resort. The hydrographic surveys showed that the bed contours are almost straight and parallel to the shoreline (Fig. 3).

The sediments along the coast west of Alexandria consist mainly of calcareous material, which originates from the limestone rocks and ridges in the sea in the project area. These sediments differ considerably from those found east of Alexandria, which originate from the Nile delta. Sediment samples at the project area were collected at different depths/locations along the coast. Also, some near shore bore holes were performed as shown in (Fig. 4). The bed samples have been found to be mainly sand which is coarse, D_{50}= (0.3-0.7) mm, in the upper part of the coastal profile. On the other hand, the median particle size of the sand is somewhat smaller, D_{50}= 0.2-0.3 mm, in the deeper part at water depths greater than 2 m below MSL. However, with some samples, rocks and gravel were observed that required simulating a fixed bed in the modeled area.

The wave data were measured during 2001-2005 with a wave gauge that belongs to the El-Dekhila Port Station and is located at a water depth of 13m. The wave data were statistically analyzed to obtain the representative wave conditions. The significant wave conditions (all year) are presented in (Table 1). It is clear that the

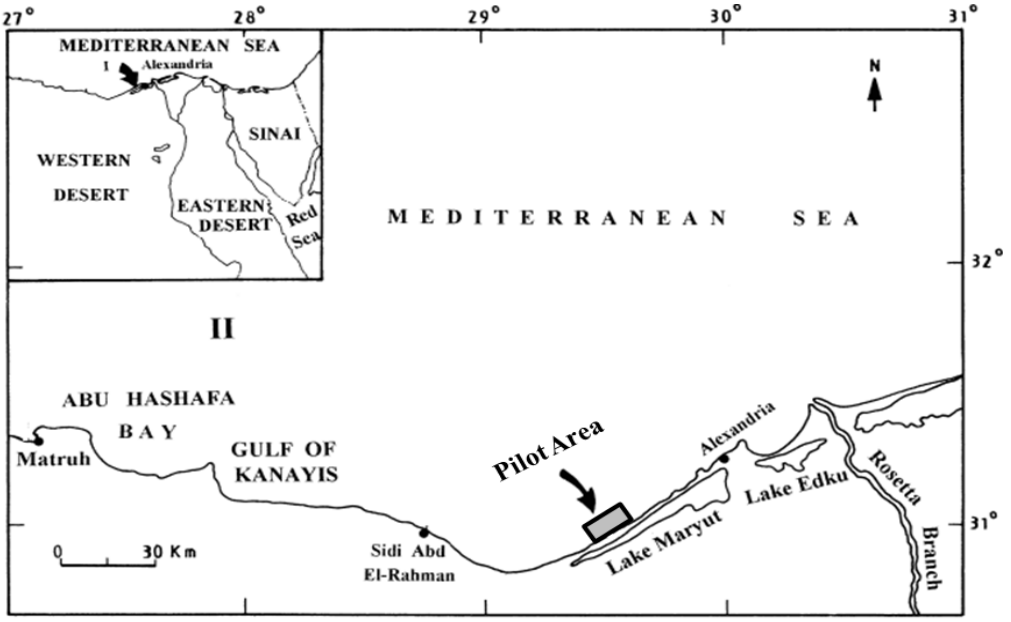

Fig. 1. Location map of the pilot area

Fig. 2. Satellite image of the project area along the North-West coast of Alexandria

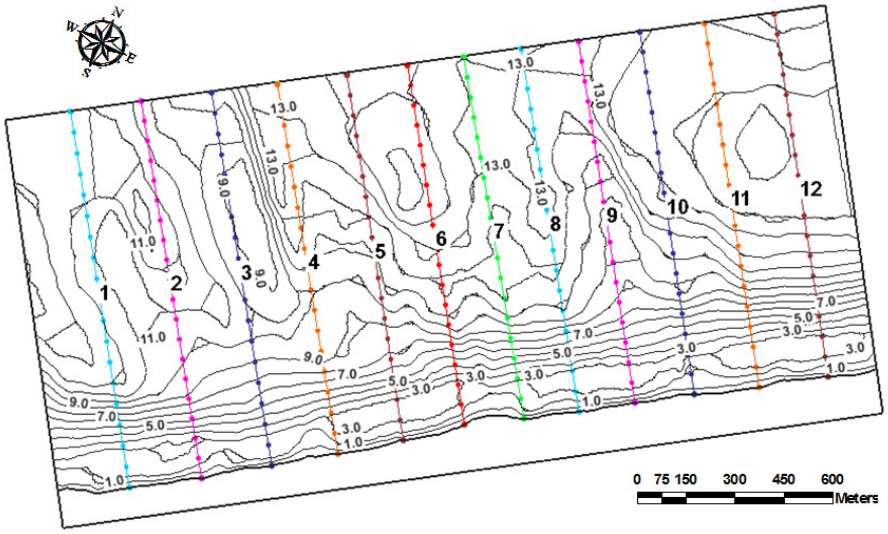

Fig. 3. Bathymetric survey in the study area in 2009

prevailing direction is North-West which is common along the Egyptian Mediterranean Coast.

The distribution of the deep water wave energy (m^2/Hz) versus the direction angle measured from the normal to the shore line during the occurrence of maximum incident wave height (Hmax.=4.6m) is shown in (Fig. 5-a).

It can be observed that most of the wave energy is centered about the normal to the shoreline and the maximum is reached at about 18 degrees to the normal on the shoreline. Also, the distribution of the deep water wave energy versus the frequency and the spectral energy distributions during the occurrence of maximum incident wave height are shown in (Figs. 5-b and 5-c), respectively. It can be observed that the maximum deep water wave energy is 36 m^2/Hz approximately.

Fig. 4. The bore holes implementation in the site

Table 1. The significant wave conditions at a water depth of 13m in El-Dekhila Port (2001-2005)

Wave condition	Hs (m)	T (s)	Direction (°N)	Duration (days/yr)
1	0.45	5	35	60.31
2	0.45	5	286	89.74
3	0.45	5	330	94.44
4	0.45	5	360	81.37
5	1.77	7	286	3.523
6	1.77	7	330	7.96
7	1.77	7	360	17.88
8	3.34	9	330	3.33
9	5.19	10	330	1.44

2.1 SMS Model

SMS is a finite difference model originally developed by Brigham Young University 1985 in cooperation with the U.S. Army Corps of Engineers, Engineer Research and Development Center (ERDC), and the U.S. Federal Highway Administration (FHWA). The SMS model adopts GENESIS (GENEralize model for SImulating Shoreline changes) based on the one-line theory for sediment transport calculations [3].

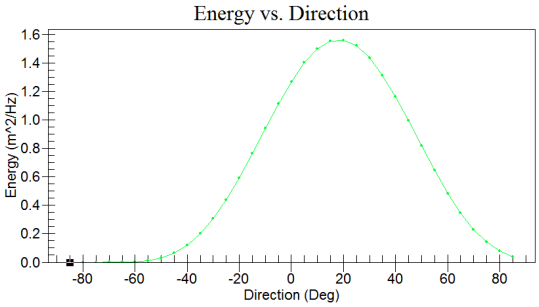

Fig. 5-a. Wave energy distribution versus the direction angle (Hmax.=4.6m)

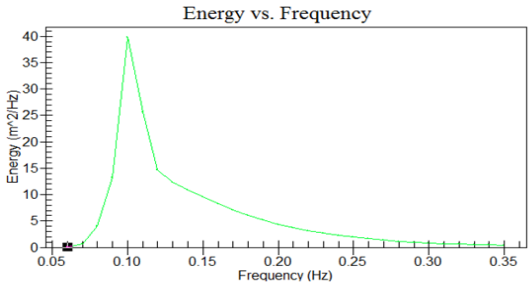

Fig. 5-b. Wave energy distribution versus frequency (Hmax.=4.5m)

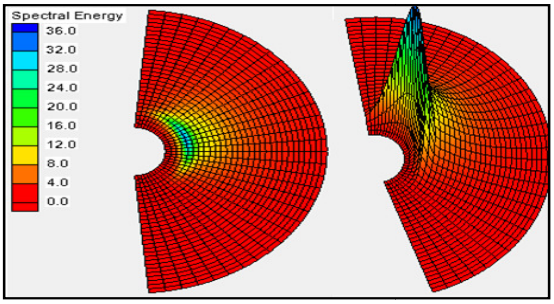

Fig. 5-c. Spectral energy distributions (Hmax.=4.5m)

Wave models in SMS include CMS-Wave, and BOUSS-2D and include both spectral and wave transformational models. Numerical wave models BOUSS-2D and CMS-Wave may be used together (coupled) to evaluate potential alternatives of coastal planning for various coastal conditions. CMS-Wave [4,5,6] is part of the Coastal Modeling System (CMS) for simulating combined waves, currents, sediment transport, and morphology change at coastal inlets, estuaries, and river mouths [7]. The CMS-Wave is a spectral wave model belonging to the phase-averaged class. It is commonly based on Energy Balance equation. It performs steady-state spectral transformation of directional random waves co-existing with ambient currents in the coastal zone. The model simulates half-plane and full-plane wave propagation, so that wave generation, wave reflection and bottom frictional dissipation of multi-directional waves can be considered. BOUSS-2D is a two dimensional (2-D) phase-resolving wave model that employs a time-domain solution of fully nonlinear Boussinesq-type equations for waves propagating in water of variable depth. The theoretical background and user manuals for BOUSS-2D are available in CMS technical reports and CHETNs [8,9].

In the present study, the GENESIS model is chosen for the simulation of the shoreline changes and evaluate the sediment rate. A one-dimensional model approach is preferred due to the facts that this type of models have wide ranged applicability in temporal and spatial scales, requires less detailed input data and computer time and may give both qualitatively and quantitatively acceptable results which may be used for both engineering and scientific purposes.

Based on the bathymetric survey, rectilinear grids have been generated and the associated depth files have been prepared for the wave models. A high grid resolution has been applied in the area of the proposed structure, and a low resolution has been implemented far away of the area of their influence. The grid cell size (5 x 5m) is fine surround the structure area and the adjacent regions while it is course (20 x 20m) in the far field till the open boundary. The model grid meets criteria for smoothness (adjacent cells do not differ much in size) and orthogonally (the angles of the comers of the cells are close to 90°), in order to avoid that small disturbances due to irregularities in the grid grow to governing features during the computation.

In order to link the modeled shoreline to the outside environment and to solve equation of the longshore sediment transport rate, the boundary conditions for either the shoreline position or the longshore sand transport at the two lateral ends of the beach are essential. Commonly applied lateral boundary conditions are Neumann or radiation boundary condition that represents the natural beach condition where the change in shoreline position is negligibly small and Dirichlet boundary condition which represents for an impermeable shore-normal barrier where sediment transport rate is equal to zero. Another type of boundary condition controls the cross-shore movement of shoreline as backward in case of seawall and as forward in case of tombolo formation behind detached breakwater.

The complete barrier lateral boundary condition can also be introduced as an internal constraint at any interior location in the grid system, to represent the applications of groins or jetties as coastal defense measures depending on their capacity of wave energy absorption and sediment transport blocking. The amount of sediment blocked by the structure is related to the seaward extent of the groin with respect to the critical offshore distance that corresponds to the depth of closure [10]. The amount of wave energy absorption capacity, which also controls the sediment blocking, is expressed as the permeability of the groin. The details of the calculations of bypassing and permeability conditions of groins in the developed model are discussed extensively by [11].

The determination of the sizes of time interval (Δt) and grid spacing (Δx) depends on the stability parameter (Rs). For small breaking wave angles, $Rs \leq 0.5$. The stability parameter gives an estimate of the numerical accuracy of the solution such that accuracy increases with decreasing values of Rs [12].

2.2 Model Input

A study has been conducted on the use of a semi-open groin for protecting a strip of the beach from severe wave attack while keeping a reasonable flushing condition and minimum shoreline changes due to the groin. The groin has been considered at 1400m from the west boundary of the study area and 1100m from the East one (Fig. 6). The groin extends for 100 m normal to the shoreline and the gap has its center midway along the groin. The average effective grain size of the soil on-site is 0.3 mm; the average berm height has been computed and found to be 1m and the closure depth is 8 m.

The wave data and bathymetric survey described in the aforementioned sections have been used to run the model for the current configurations (see Table 2) and the results have been presented, analyzed and discussed. It is noteworthy that the current investigations have been focused on the effect of the size of the gap and permeability of the groin on the wave height, radiation stresses and shoreline changes. It is also considered that wave height less than 1.0m and radiation stresses less than 0.5m/sec represent favorable conditions for swimmers around the jetty. Thus, the model output has been presented during the occurrence of maximum incident wave height (H=4.6m) to identify locations of high wave and/or radiation stresses. The impact of various groin configurations on the shoreline has been presented at the end of the simulation period of year 2012.

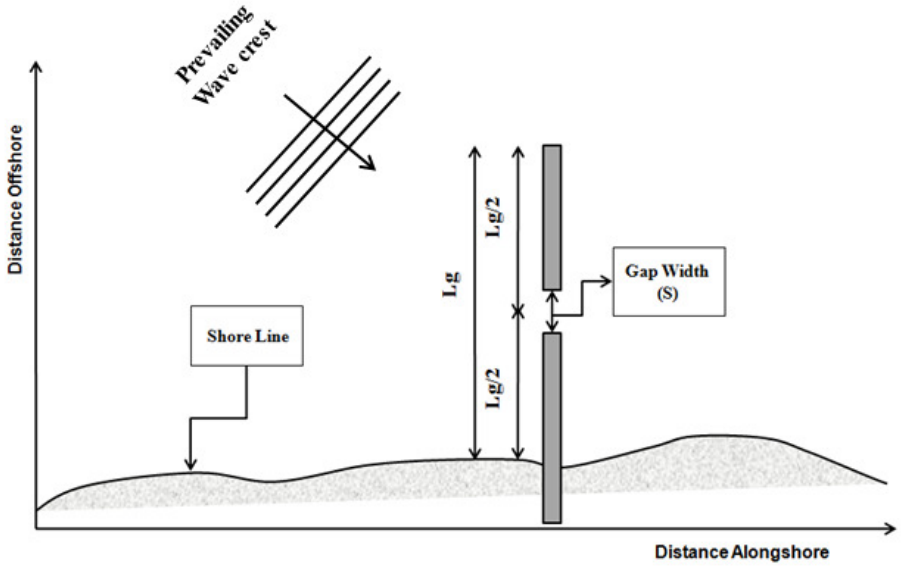

Fig. 6. Definition sketch of study

Table 2. Input parameters for the case study

Run-no.	Groin length (m)	Groin permeability	Gap width (m)	Note
1	-	-	-	No structure
2	100	0	0	No gap but variable
3	100	0.2	0	permeability of the groin
4	100	0.5	0	
5	100	0	5	Impermeable groin and
6	100	0	10	middle gap of variable size
7	100	0	15	
8	100	0	20	

2.3 Model Calibration and Validation

Based on the measured shorelines of 2007, 2009 and 2012 the model was calibrated. A comparison was prepared between the computed and measured shoreline changes (Fig. 7-a) for different cases of different calibration coefficients (K1, K2) in the longshore sediment transport formula. (Fig. 7-b) illustrate the correlation between the measured shoreline and the computed shoreline for various values of calibration coefficients. The correlation value (R2 =0.965) for K1=0.25 and K2=0.03. The correlation value (R2 =0.9935) for K1=0.35 and K2=0.06. However, the correlation value (R2 =0.9999) for K1=0.45 and K2=0.10. Thus, the best values of the calibration coefficients for the study area are K1=0.45 and K2=0.10.

The net long shore transport is estimated to be slightly north-east directed with a magnitude of 15000m^3/year approximately [13]. The longshore sediment transport were calculated based on Ozasa and Brampton formula in SMS model, and calibrated based on these amount of sediment transport. The computed net transport integrated over one year of simulation, including seabed update. The model computes the north-eastward directed net longshore transport of 5,000 to 12,000 m^3/year at the up drift boundary. The overall conclusion of the confrontation of the numerical model results with the measurements is that the numerical model is capable of simulating the shoreline changes in the pilot area.

3. RESULTS AND ANALYSIS

The SMS model has been used to simulate the wave hydrodynamics around the groin for about 5 years to study the impact of the proposed groin on the shoreline and wave conditions at various time steps. (Fig. 8-a) shows the wave direction and height as the waves approach the groin during the occurrence of maximum incident wave height within the study period, i.e., Hi=4.6 m. It can be observed that waves approach the shore normal to it due to refraction and shoaling and wave height at the tip of the groin is about 2.5 m, decreasing rapidly to about 0.5 m high as it propagates along the groin. The waves affected by the groin are within 100 m away from the groin on both sides, i.e., the same length of the groin, while the decay on the East side (up drift for the prevailing wave conditions) is slightly larger than that on the west side (down drift for the prevailing wave conditions).

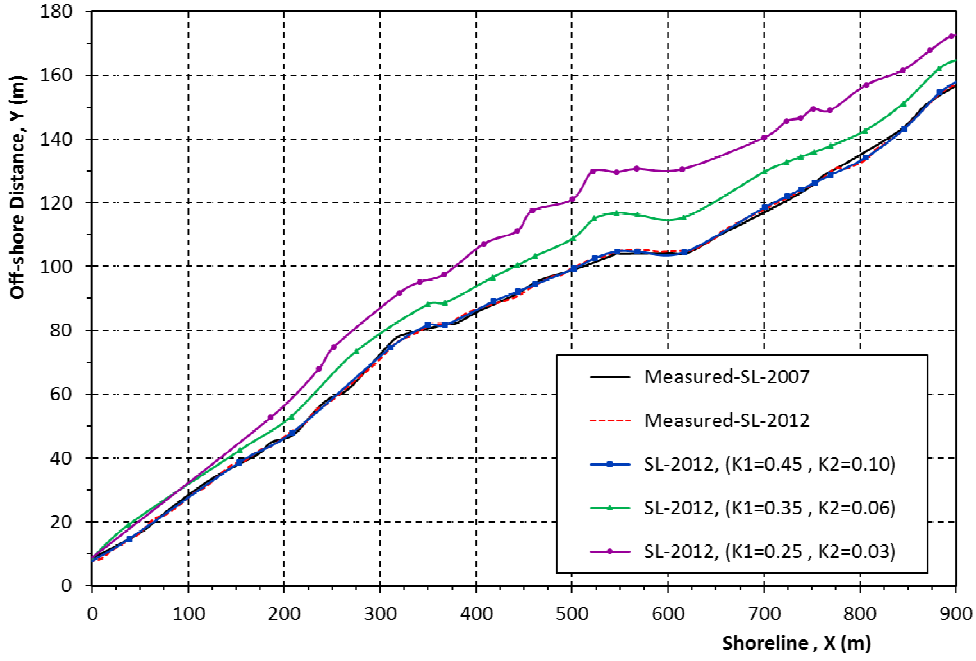

Fig. 7-a. Shoreline change rates along the coast in term of the calibration coefficients

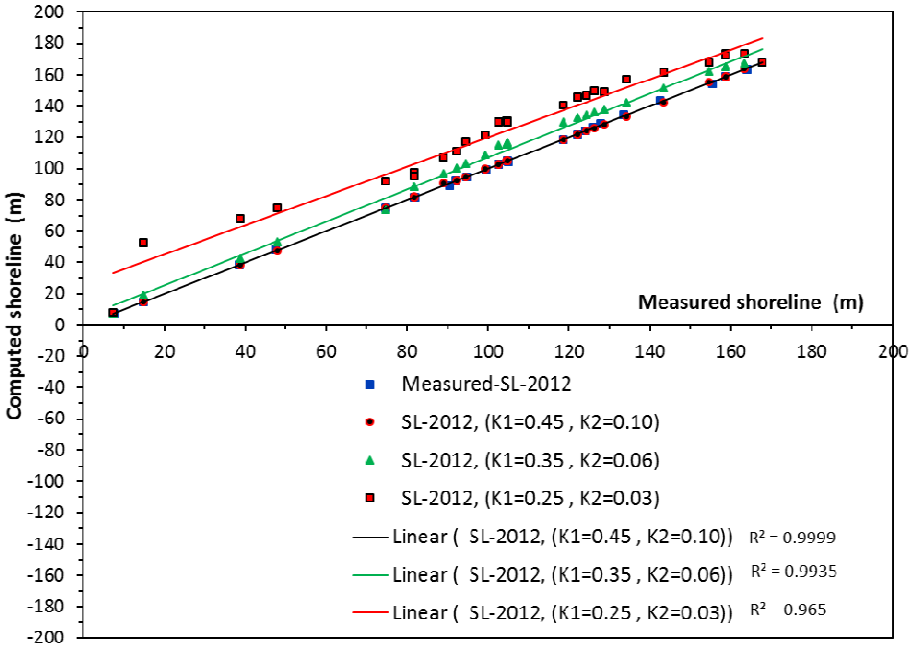

Fig. 7-b. Correlation of the shoreline change for different cases of different calibration coefficients (K1, K2)

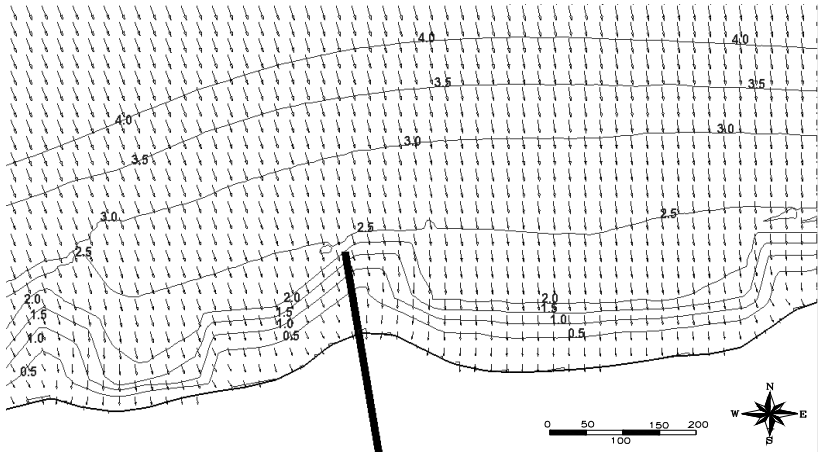

Fig. 8-a. Computed wave height (m) and direction in the vicinity of the groin during the occurrence of maximum incident deep water wave height (Hi=4.6m, Lg= 100m, P=0.0 and S/ Lg=0)

(Fig. 8-b) shows two breaker lines, i.e., one in deep water and the other in shallow water as well as breaking at the head of the groin itself. Moreover, rip current can be noticed on the up drift side and a rip head is formed offshore. The numerical results have shown that radiation stresses have been as high as 0.74 m/sec.

(Figs. 9-a and 9-b) show the case of a small gap in the middle section of the groin having a width of 0.05Lg. It can noticed that some waves cross the gap from the up drift to the lee of the groin due to the effect of wave diffraction and the wave height at the down drift side is slightly higher than the case of the no gap in the groin. Also, some currents cross the gap to the lee ward of the

groin and interact with the wave-induced current causing some turbulence.

(Figs. 10 through 12) show the cases of larger gaps varying in size from S/Lg=0.10 and 0.20 and almost the same trend can still be observed, i.e., slight increase in wave height, more currents crossing the gap and less turbulence inside the gap. It is observed that the offshore zone of the groin is almost unaffected by the gap in the groin, but the effect of the gap is evident on the lee ward of the groin. It can be observed that the case of large gap (S/Lg=0.2) shows minor impact of the groin in protecting its leeward from waves and the waves on both sides of the groin have nearly equal heights.

Investigations have also been made for the effect of groin permeability on the wave height and radiation stresses in the vicinity of the groin. The results have been presented in (Figs. 13 and 14) during the occurrence of maximum incident wave height as a sample output of the simulation results. It can be seen that the larger the permeability of the groin is, the less the protection of the leeward zone from wave attack becomes. It is also noticed that some currents cross the groin from one side to the other due to the permeability of the groin. Also the wave heights on both sides of the groin are almost the same for the case of P=0.5. The effect of the permeability is more evident in the case of P=0.5 (Fig. 14) than in the case of P=0.2 (Fig. 13). It can be stated that the permeable groin provides good circulation of flow while keeping reasonable protection of the groin on the leeward side from wave attack. It is also anticipated that the current carries sediments through the groin as the current passes the groin. Thus, the impact of the groin on shoreline changes becomes less as the groin has larger permeability.

Investigations have been made for the impact of the gap width on the shore line changes in the close vicinity of the groin. It is noteworthy that most of coastal protection structures, e.g., breakwaters and groins, have been recently rejected by the Egyptian Environmental Affairs Agency (EEAA) due to their adverse impact on the shoreline that usually extends to the surrounding villages. Some villages even suffer from nearly complete erosion of their sand beach due to the construction of detached breakwaters on the up drift side, e.g., Marabella and Suez Canal resorts.

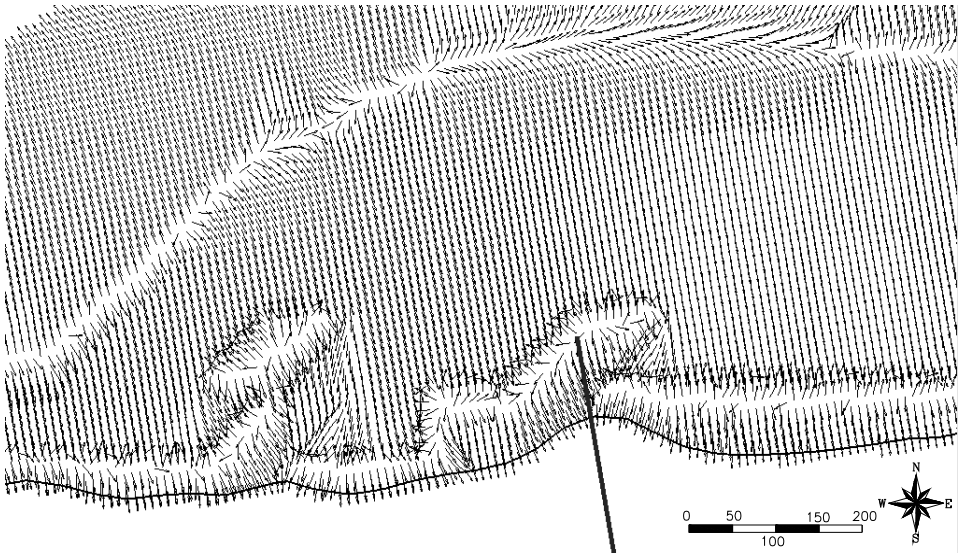

Fig. 8-b. Computed radiation stress (m/sec) during the occurrence of maximum incident deep water wave height in the vicinity of the groin (Hi=4.6m, Lg=100m, P=0.0 and S/ Lg=0)

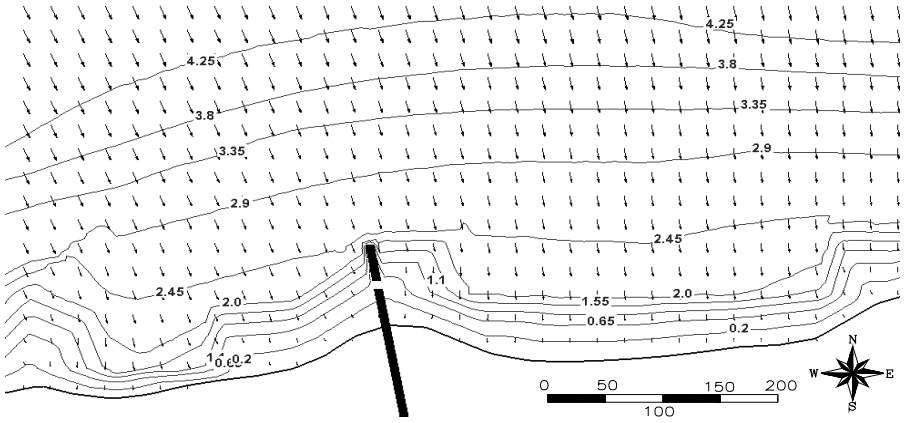

Fig. 9-a. Computed wave height and direction during the occurrence of maximum incident deep water wave height in the vicinity of the groin (Hi=4.6m, Lg= 100m, P=0.0 and S/ Lg=0.05)

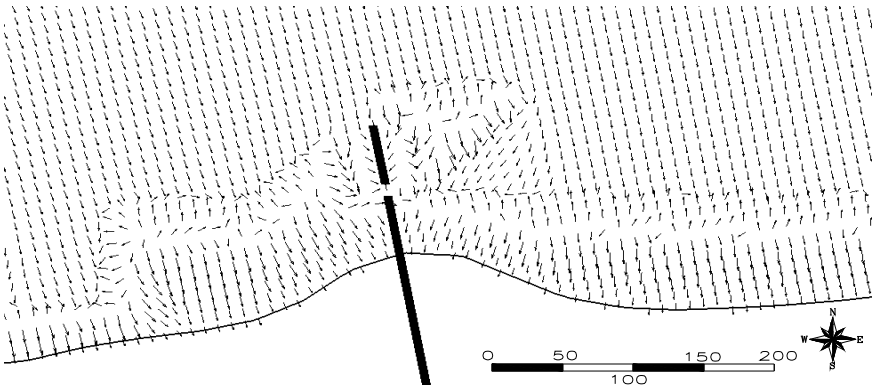

Fig. 9-b. Computed radiation stress (m/sec) during the occurrence of maximum incident deep water wave height in the vicinity of the groin (Hi=4.6m, Lg= 100m, P=0.0 and S/ Lg=0.05)

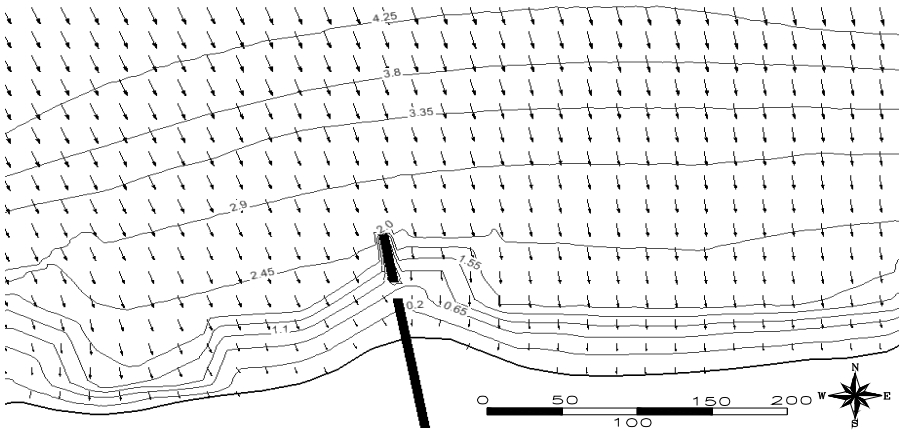

Fig. 10. Computed wave height and direction during the occurrence of maximum incident deep water wave height in the vicinity of the groin (Hi=4.6m, Lg= 100m, P=0.0 and S/ Lg=0.10)

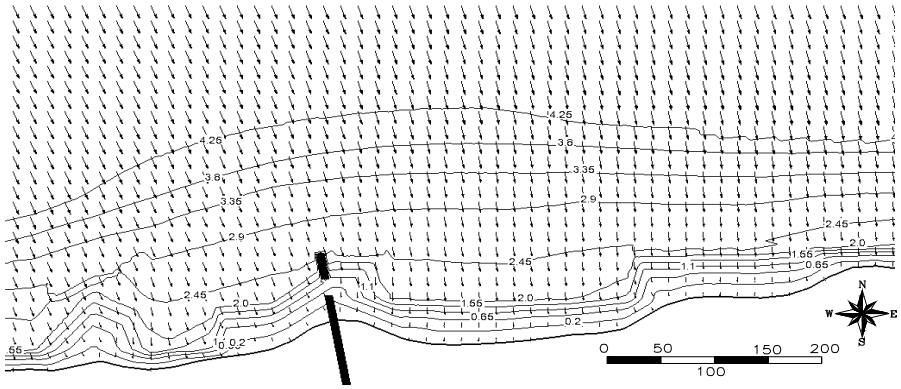

Fig. 11. Computed wave height and direction during the occurrence of maximum incident deep water wave height in the vicinity of the groin (Hi=4.6m, Lg= 100m, P=0.0 and S/ Lg=0.15)

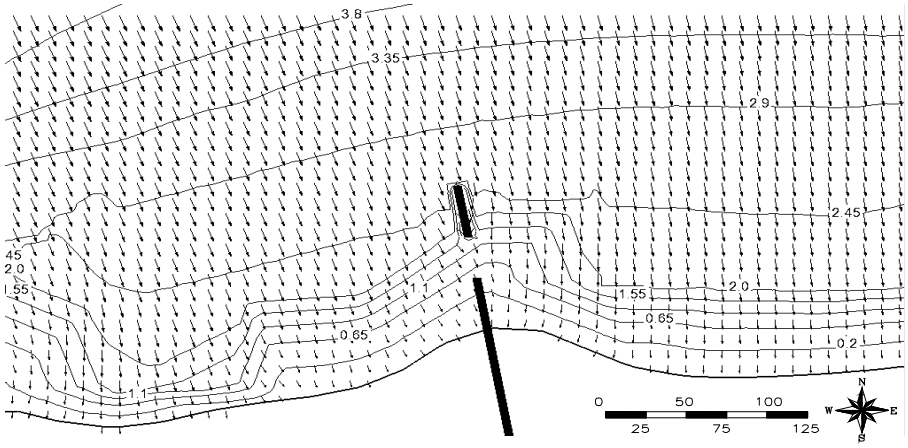

Fig. 12. Computed wave height and direction during the occurrence of maximum incident deep water wave height in the vicinity of the groin (Hi=4.6m, Lg= 100m, P=0.0 and S/Lg=0.20)

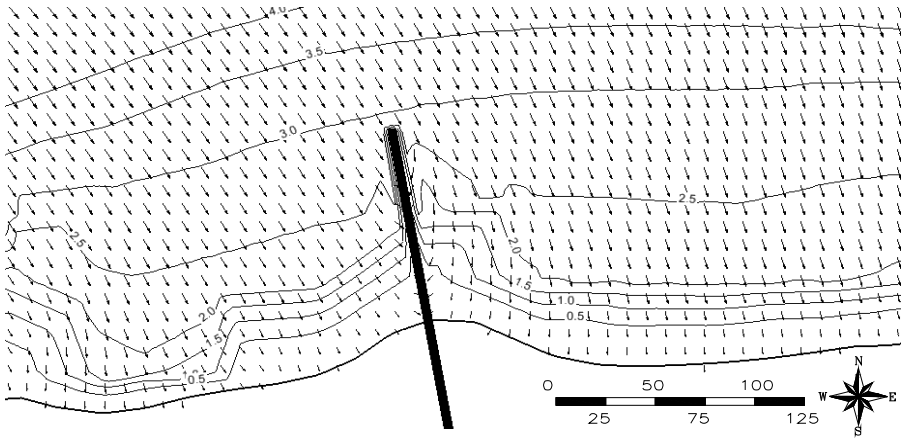

Fig. 13. Computed wave height and direction in the vicinity of the groin during the occurrence of maximum incident deep water wave height (H_i=4.6m, L_g=100m, P=0.2 and S/ L_g=0)

(Figs. 15-a through 15-d) show the computed and measured shoreline changes along the shoreline due to various size of the gap while the groin is impermeable after one year from the groin construction. It can be observed that there are small differences between the computed and measured shoreline changes along the up drift and down drift of the groin. Correlation of the computed and measured shoreline changes is illustrated in (Fig. 16).

(Fig. 17) shows the shoreline changes along the shoreline due to various sizes of the gap while the groin is impermeable after one year from construction. It also shows the case of no groin is constructed for comparison with the case of the groin. It can be seen that considerable changes have occurred in the shoreline very close to the groin, but the changes due to the groin are limited to some distances away from the groin. The latter distance is called the effective length of the groin on the shoreline.

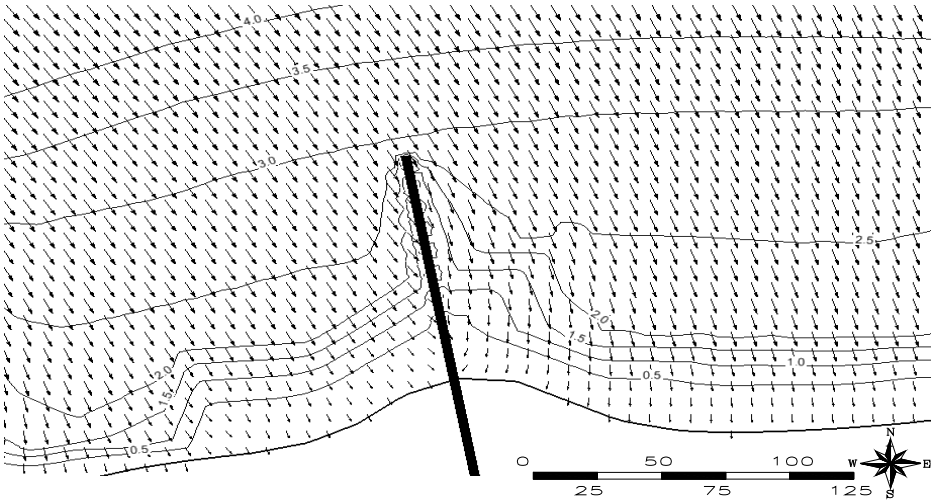

Fig. 14. Computed wave height and direction in the vicinity of the groin during the occurrence of maximum incident deep water wave height (H_i=4.6m, L_g= 100m, P=0.5 and S/ L_g=0)

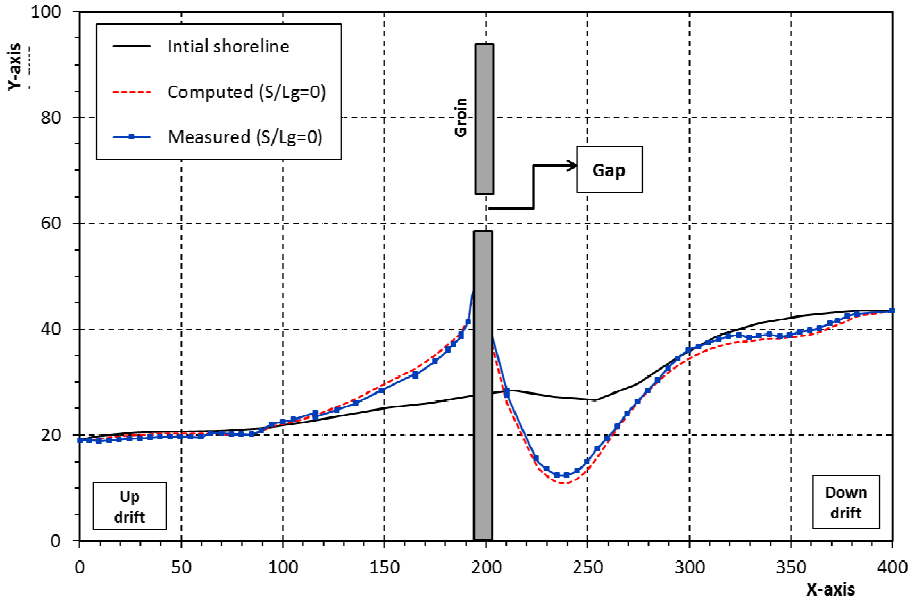

Fig. 15-a. Computed and measured shoreline changes along the coast (L_g=100m, S/Lg=0)

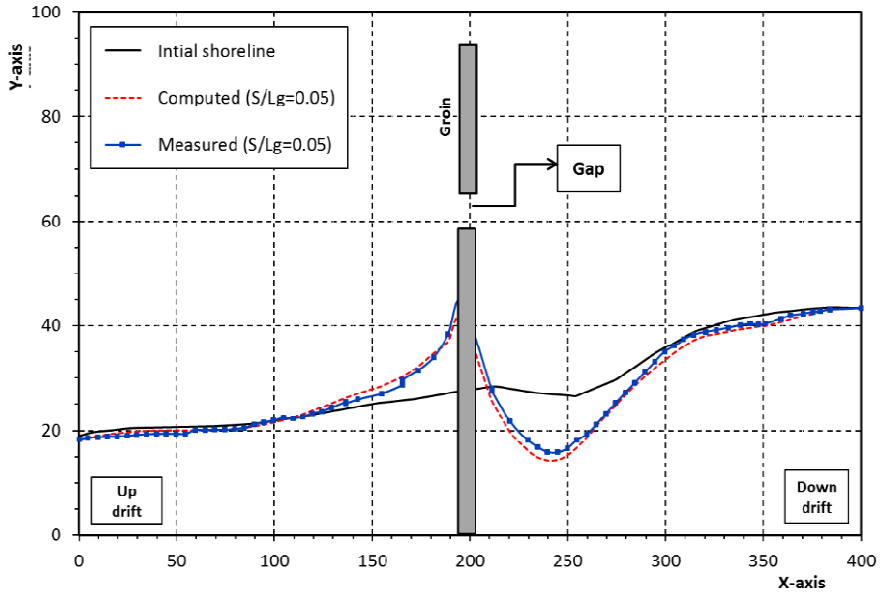

Fig. 15-b. Computed and measured shoreline changes along the coast (L_g=100m, S/Lg=0.05)

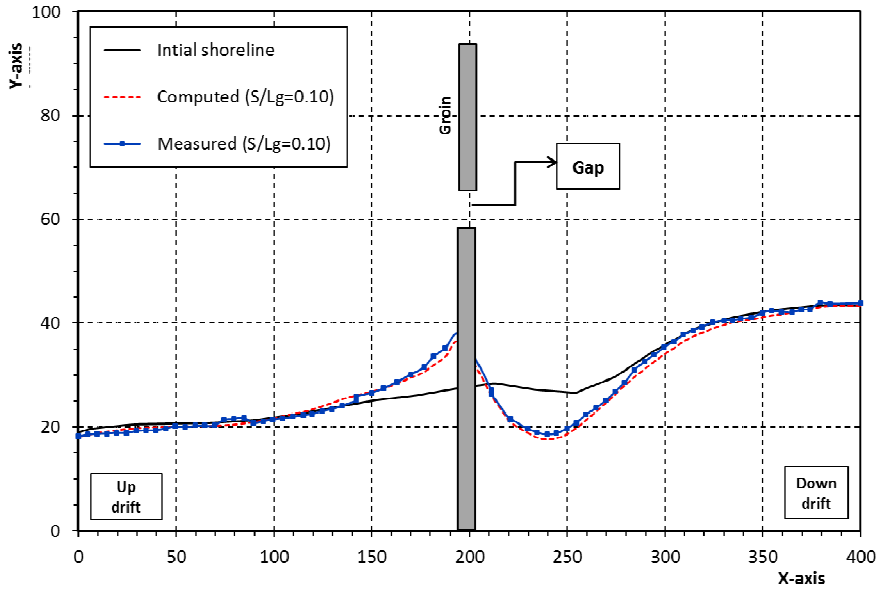

Fig. 15-c. Computed and measured shoreline changes along the coast (L_g=100m, S/Lg=0.10)

Of course, the shoreline away from this length is still affected by direct wave attack, but without being affected by the groin. It can be seen that accretion occurs at the up-drift side and scour develops on the down drift one. It should be remarked that the prevailing wind direction is at the right hand side of the groin while the direction of occurrence of maximum wave height is at its left hand side. The case of no groin shows that the location of the groin could be subject to scour if the groin were not constructed. However, erosion increases on the down-drift side, but accretion takes place on the up-drift side after the jetty is constructed.

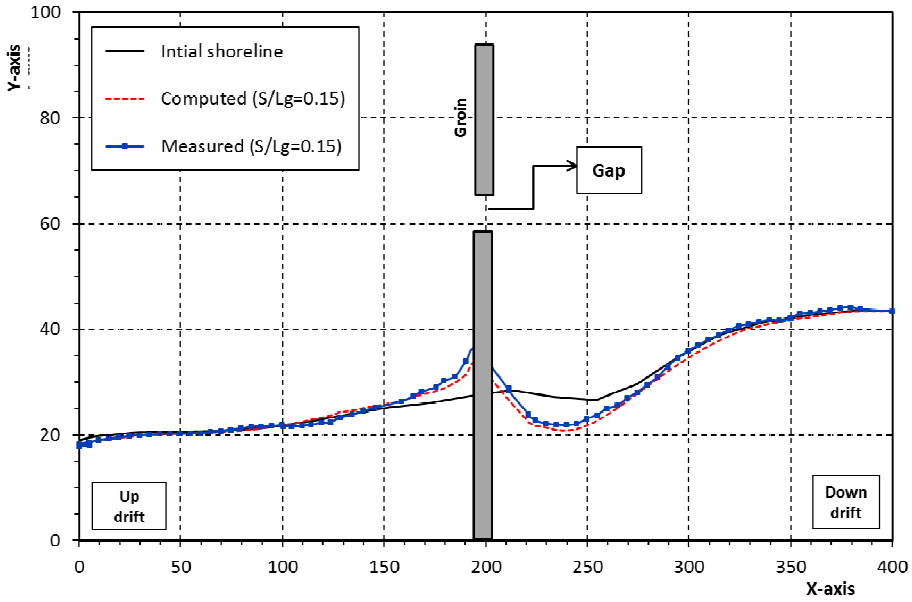

Fig. 15-d. Computed and measured shoreline changes along the coast (L_g=100m, S/Lg=0.15)

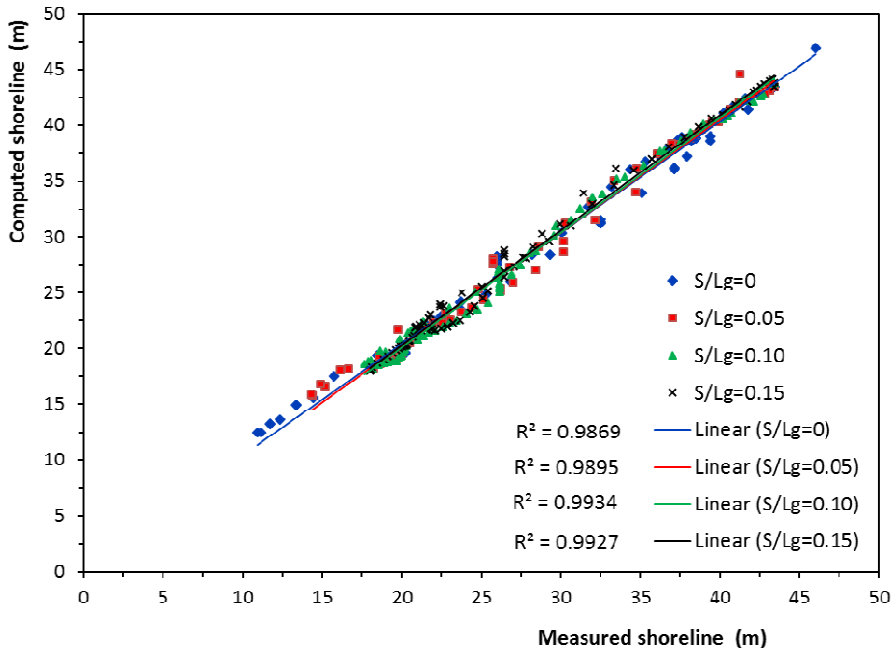

Fig. 16. Correlation of the computed and measured shoreline changes

(Fig. 18-a) shows that the erosion is generally slightly larger than accretion. The maximum scour depth varies from 0.16 Lg for the case of no gap to as small as 0.06 Lg if S=0.15 Lg. Also noticed is that the maximum scour and deposition depths are almost equal in case of S=0.15Lg. On the other hand, the variation of maximum scour/deposition depth varies almost linearly against the gap width. However, this result could not be generalized for all cases unless further investigations are made to confirm the relation.

Fig. 18-b) shows the variation of the length of the affected zone of the groin versus the gap width. It is clear that the up drift is much more impacted by the groin as compared with the down drift for the cases investigated in this work. The up drift is affected up to twice the length of the groin in case of no gap and the length is about 1.1 Lg in case the gap width equals 0.15 Lg. The variation of the effective length on the down drift varies slowly as the gap width varies, i.e., varies from 1.2 to 1.1 as S/Lg varies from 0 to 0.15. It is noteworthy that the variation of the effective length is nearly linear with the gap width in this study.

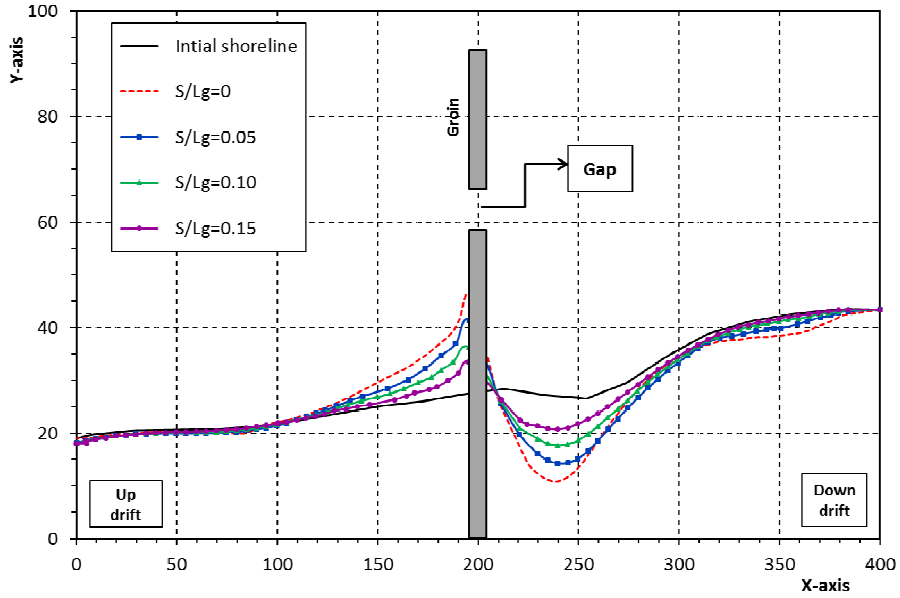

Fig. 17. Computed shoreline changes along the coast for various gap widths during the period 2010-2014 (L_g=100m, P=0.0)

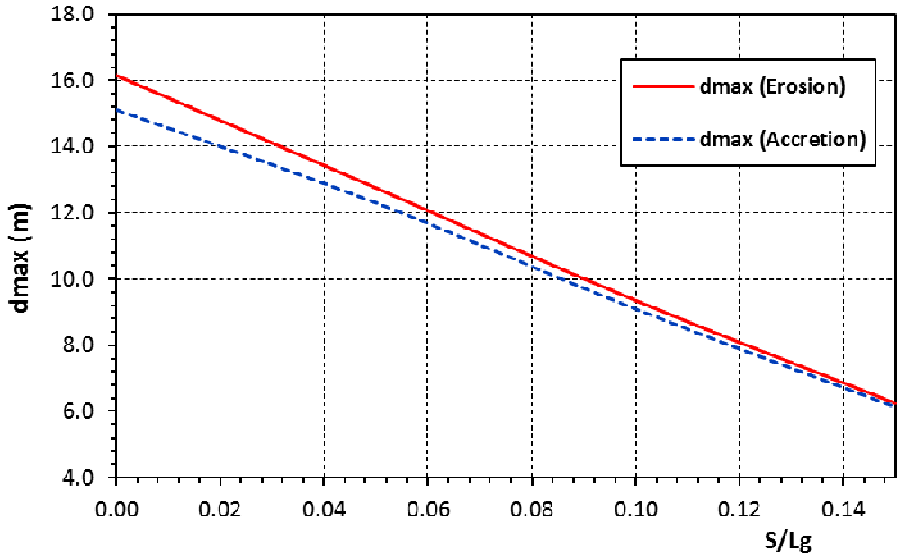

Fig. 18-a. Computed maximum depth of erosion/accretion along the shoreline for various gap width during the period 2000-2005 (L_g= 100m, P=0.0)

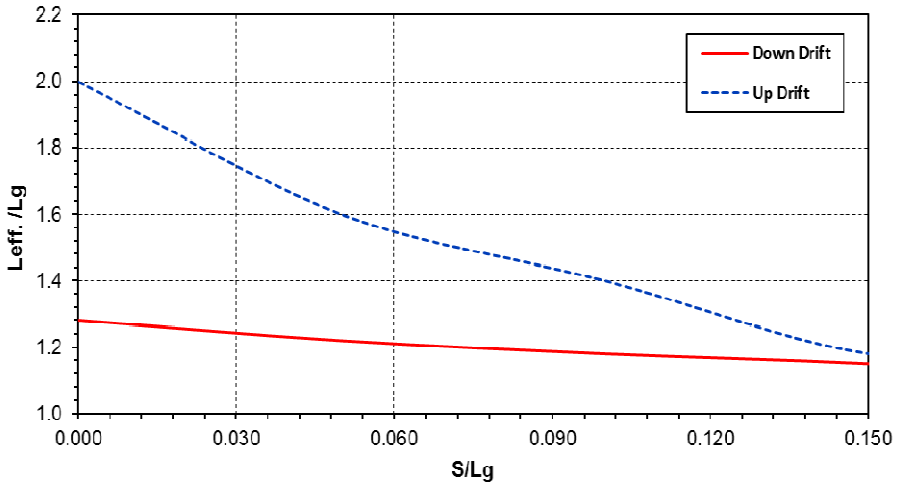

Fig. 18-b. Computed effective length along the shoreline for various gap width during the period 2000-2005 (L_g= 100m, P=0.0)

4. CONCLUSION

A study has been conducted to investigate a clear opening in the groin cross section on the wave height, currents and shoreline changes in the vicinity of the groin. This investigations aims at providing some guidelines for the design of the groin if safe swimming conditions are sought and shoreline changes are of major concern. The followings have been concluded:

- Groins can be a good tool to provide safe swimming conditions along the North-West coast of Egypt if they are properly designed and studied.
- The permeability of the groin allows the flow of water across the groin and better flushing in the leeward of the groin. It also reduces the shoreline changes due to the construction of the jetty.
- The gap in the groin also allows better circulation of water between both sides of the groin and reduces the shoreline changes. It has been found that gaps larger than 0.15 of the groin length have almost the same impact of a single groin (the onshore part), while the offshore part becomes of minor impact on the shoreline changes.
- It is found that the maximum erosion and accretion depths are almost equal in case of S>0.15 Lg for the cases investigated.
- The effective length on the up-drift side is much more than that on the down-drift for the cases investigated in this work. The up-drift is affected up to twice the length of the groin in case of no gap and the length is about 1.1 Lg in case of gap width equals 0.15 Lg.
- The variation of the effective length on the down-drift varies slowly as the gap width varies. The effective length varied from 1.2 to 1.1 as S/Lg varies from 0 to 0.15. It is noteworthy that the variation of the effective length is nearly linear with the gap width in this study.
- In the present study, the impacts of the gap has its center midway along the groin have been investigated. Thus, it is recommend to study the gab location/width impacts.

COMPETING INTERESTS

Authors have declared that no competing interests exist.

REFERENCES

1. MOH. El-Alamein Marina resort erosion study, a report prepared by delft hydraulics to the Ministry of Housing, Utilities and Urban Communities of Egypt; 2000.
2. WLIDelft Hydraulics. Integrated development of Egypt's Northwestern Coastal Zone, development of near shore water conditions, a report prepared by Delft Hydraulics to the Ministry of Water Resources and Irrigation of Egypt; 2002.
3. Hanson H. GENESIS: A generalized shoreline change numerical model for engineering Use, Ph.D. Thesis, University of Lund, Lund, Sweden; 1987.

4. Lin L, Demirbilek Z, Yamada F. CMS-Wave: A near shore spectral wave processes model for coastal inlets and navigation projects, Coastal and Hydraulics Laboratory Technical Report ERDC/CHL TR-08-13. Vicksburg, MS: U.S. Army Engineer Research and Development Center; 2008.
5. Lin L, Demirbilek Z, Mase H. (2011), "Recent capabilities of CMS-Wave: A coastal wave model for inlets and navigation projects, proceedings, symposium to honor Dr. Nicholas Kraus. Journal of Coastal Research. 2011;(59):7-14.
6. Demirbilek Z, Lin L, Zundel A. WABED model in the SMS, Coastal and Hydraulics Laboratory Engineering Technical Note ERDC/CHL CHETN-I-74. Vicksburg, MS: U.S. Army Engineer Research and Development Center; 2007.
7. Demirbilek Z, Rosati JD. Verification and validation of the coastal modeling system, Report I, Executive Summary. Tech. Report ERDC/CHL-TR- 11-xx. Vicksburg, MS: U.S. Army Engineer Research and Development Center; 2011.
8. Demirbilek Z, Zundel A, Nwogu O. BOUSS-2D wave model in SMS: I. Graphical Interface", Tech. Note ERDC/CHL-I-69, U.S. Army Engineer R&D Center Vicksburg, MS; 2005.
9. Nwogu O, Demirbilek Z. BOUSS-2D: A Boussinesq wave model for coastal regions and harbors, Coastal and Hydraulics Laboratory Technical Report ERDC/CHL TR-01-25. Vicksburg, MS: U.S. Army Engineer Research and Development Center; 2001.
10. Dabees MA, Kamphus JW. NLINE; Efficient Modeling of 3-D Beach Change. 25th international Conference on Coastal Engineering, Sydeny-Australia. 2000;2700-2713.
11. Şafak I. Numerical modeling of wind wave induced longshore sediment transport, M.S. Thesis, METU, Ankara; 2006.
12. Hanson H, Kraus NC. Seawall boundary condition in numerical models of shoreline evolution, Technical Report CERC-86-3, U.S. Army Engineer Waterways Experiment Station, Vicksburg, MS; 1986.
13. WL|Delft Hydraulics. Integrated Development of Egypt's Northwestern Coastal Zone, Development of Near Shore Water Conditions. Report H3791; 2004.

Peer-review history:
The peer review history for this paper can be accessed here:
http://www.sciencedomain.org/review-history.php?iid=756&id=31&aid=6988